



Published in final edited form as:

Wound Repair Regen. 2013 May ; 21(3): 473–481. doi:10.1111/wrr.12039.

A Modified Collagen Gel Enhances Healing Outcome in a Pre-Clinical Swine Model of Excisional Wounds

Haytham Elgharably, MD, Sashwati Roy, PhD, Savita Khanna, PhD, Motaz Abas, BS, Piya DasGhatak, MS, Amitava Das, MS, Kareem Mohammed, MD, and Chandan K. Sen, PhD

Departments of Surgery, Davis Heart & Lung Research Institute, Center for Regenerative Medicine and Cell based Therapies and Comprehensive Wound Center, The Ohio State University Wexner Medical Center, Columbus, Ohio

Abstract

Collagen-based dressings are of great interest in wound care. However, evidence supporting their mechanism of action in a wound setting *in vivo* is scanty. This work provides first results from a pre-clinical swine model of excisional wounds elucidating the mechanism of action of a modified collagen gel (MCG) dressing. Following wounding, wound-edge tissue was collected at specific time intervals (3, 7, 14, and 21 days post-wounding). On day 7, histological analysis showed significant increase in the length of rete ridges suggesting improved biomechanical properties of the healing wound tissue. Rapid and transient mounting of inflammation is necessary for efficient healing. MCG significantly accelerated neutrophil and macrophage recruitment to the wound site on day 3 and day 7 with successful resolution of inflammation on day 21. MCG induced MCP-1 expression in neutrophil-like HL-60 cells *in vitro*. *In vivo*, MCG treated wound tissue displayed elevated VEGF expression. Consistently, MCG-treated wounds displayed significantly higher abundance of endothelial cells with increased blood flow to the wound area indicating improved vascularization. This observation was explained by the finding that MCG enhanced proliferation of wound-site endothelial cells. In MCG-treated wound tissue, Masson's Trichrome and Picrosirius red staining showed higher abundance of collagen and increased collagen type I:III ratio. This work presents first evidence from a pre-clinical experimental setting explaining how a collagen-based dressing may improve wound closure by targeting multiple key mechanisms as compared to standard of care i.e., Tegadem treated wounds. The current findings warrant additional studies to determine whether the responses to the MCG are different from other modified or unmodified collagen based products used in clinical setting.

INTRODUCTION

Chronic ulcers represent a major clinical challenge to wound care providers. Patients suffering from non-healing ulcers are prone to serious complications such as secondary infection and amputation which are associated with high rates of mortality (1). Chronic wounds pose a substantial burden on the health system in the United States with \$5–10 billion being spent annually for management of these wounds (2). The development of effective and clinically relevant therapeutic interventions thus represents a matter of high priority.

Address correspondence to: Chandan K. Sen, PhD 473 West 12th Avenue, 512 DHLRI The Ohio State University Medical Center Columbus, Ohio 43210 Tel. 614 247 7658; Fax 614 247 7818 chandan.sen@osumc.edu.

Conflict Disclosure: The work was partly supported by Southwest Technologies Inc. by means of an unrestricted gift where the donor had no control over scientific experiments or reporting.

The extracellular matrix (ECM) is a key compartment in the healing tissue. In addition to providing structural support to the healing tissue, the ECM elicits cell signaling aimed at executing the healing response(3). Fibrillar collagen represents the most abundant interstitial ECM of the skin representing 25-35% of the whole-body protein content. The three-dimensional collagen architecture defines mechanical tissue properties, *i.e.* stiffness and porosity, which guide or oppose cell migration and positioning in different contexts, such as regeneration and immune response. Because of such properties, collagen-based dressings have been of interest in wound care(4). In addition to being an inducer of cell signaling, collagen-based dressings may improve healing outcomes by deactivating excessive matrix metalloproteases by acting as a sacrificial substrate(5). Collagen dressings may also recruit several cell types to the wound site facilitating granulation tissue formation. Furthermore, such dressings may help maintain moist wound environment by absorbing wound exudates (6). Several efforts are currently in progress to optimize the composition and formulation of collagen dressings(4). In this work, we elucidate the mechanism of action of a gel formulated to produce a highly concentrated dispersion of modified collagen.

MATERIALS AND METHODS

Swine Excisional Wound Model and Treatment

Domestic white pigs were used in this study. All experiments were approved by the Ohio State University Institutional Laboratory Animal Care and Use Committee (ILACUC). Pigs (70–80 lb) were sedated by Telazol and anesthetized by mask with isoflurane (3-4%). The dorsal region was shaved. The skin was surgically prepared with alternating chlorhexidine 2% and alcohol 70% (Butler Schein, Columbus, OH) scrubs. Under such aseptic conditions, four sets of full thickness excisional wounds were established on the back of pigs using a 3 mm disposable biopsy punch. The depth of the wound is measured by the length of stainless steel section of the punch biopsy (7 mm). The wounds were created by cutting through the skin until the entire length of the stainless steel section is below the skin and the plastic shoulders (edges) are at the surface of the skin, with that length being enough to reach the subcutaneous fat in all wounds. A total of 4 sets with 8 wounds in each set were created on each side of the back (Fig 1). A scaled plastic template was used to create the wounds at fixed distance from each other and from the spine (4 cm), starting below the lower border of the scapula on the dorsum of the pig. Wounds from one side of the back were treated with a modified collagen gel (MCG) followed by dressing with Tegaderm™ (3M™, St. Paul, MN) while the wounds from the contralateral side of the back were dressed with Tegaderm™ only and received no other treatment (control). In all pigs, control & treated wounds were created on different sides in same animal, with all applications to the wounds maintained constant, ensuring exposure to similar biological effects. Treatment sides were alternated among the animals to avoid any side-specific effect. Wounds of the treatment side were retreated with MCG at 24h and 72h post-wounding. On specified time points (day 3, 7, 14, 21 post-wounding), the entire wound tissue was harvested using a 6 mm disposable biopsy punch for subsequent analyses. Animals were maintained on 12h light – dark cycles and were euthanized after the completion of experiments. MCG was provided as Stimulen™ gel by Southwest Technologies Inc. (North Kansas City, MO)(7, 8). According to the manufacturer, the unique formulation of the MCG represents a mixture of 52% collagen of long and short polypeptides along with glycerine, water and fragrance. The MCG is a highly concentrated modified collagen (mainly type I) in a gel form. We performed a proteomics analysis to determine the components present in the MCG.

Proteomic Analysis

Sample preparation and MS analysis—Proteins/peptides in MCG were purified using SDS PAGE. After tryptic digestion of the purified proteins, the MS/MS spectra were

obtained using capillary-liquid chromatography tandem mass spectrometry (Cap-LC/MS/MS). A Thermo Finnigan LTQ mass spectrometer equipped with a CaptiveSpray source (BrukerMichrom Billerica, MA) in positive ion mode was used. The LC system was an UltiMate™ 3000 system from Dionex (Sunnyvale, CA). The solvent A was water containing 50mM acetic acid and the solvent B was acetonitrile. 5 µL of each sample was first injected on to the µ-Precolumn Cartridge (Dionex, Sunnyvale, CA), and washed with 50 mM acetic acid. The injector port was switched to inject and the peptides were eluted off of the trap onto the column. A 0.2×150mm, 3µ, 200Å, Magic C18 (BrukerMichrom Billerica, MA) was used for chromatographic separations. Peptides were eluted directly off the column into the LTQ system using a gradient of 2-80%B over 45 minutes, with a flow rate of 2µl/min. The total run time was 65 minutes. The MS/MS was acquired according to standard conditions established in the lab. Briefly, a CaptiveSpray source operated with a spray voltage of 3 KV and a capillary temperature of 200°C is used. The scan sequence of the mass spectrometer was based on the TopTen™ method; the analysis was programmed for a full scan recorded between 350 – 2000 Da, and a MS/MS scan to generate product ion spectra to determine amino acid sequence in consecutive instrument scans of the ten most abundant peak in the spectrum.

Data processing and analysis—Sequence information from the MS/MS data was processed by converting the .raw files into a merged file (.mgf) using an in-house program, RAW2MZXML_n_MGF_batch (merge.pl, a Perl script). The resulting mgf files were searched using Mascot Daemon by Matrix Science version 2.3.2 (Boston, MA) and the database searched against the full SwissProt database version 2012_06 (536,489 sequences; 190,389,898 residues) or NCBI database version 20120515 (18,099,548 sequences; 6,208,559,787 residues). The mass accuracy of the precursor ions were set to 1.8 Da and the fragment mass accuracy was set to 0.8 Da. Considered variable modifications were methionine oxidation and deamidation (NQ). Fixed modification for carbamidomethyl cysteine was considered. Two missed cleavages for the enzyme were permitted. A decoy database was searched to determine the false discovery rate (FDR) and peptides were filtered according to the FDR and proteins identified required bold red peptides. Protein identifications were checked manually and proteins with a Mascot score of 50 or higher with a minimum of two unique peptides from one protein having a -b or -y ion sequence tag of five residues or better were accepted and have been presented in Table 1.

Histology—Formalin-fixed paraffin-embedded or optimum cutting temperature (OCT)-embedded frozen wound-edge specimens were sectioned. The paraffin sections were deparaffinized and stained with hematoxylin& eosin (H&E), Masson's trichrome, or Picrosirius red staining using standard procedures. Immunohistochemical staining of paraffin or frozen sections was performed using the following primary antibodies: Keratin 14 (1:600; K14; Thermo Fisher Scientific Inc., Waltham, MA), DAPI (1:10000; Life Technologies™, Grand Island, NY), anti-Myeloperoxidase (1:400; Dako North America Inc., Carpinteria, CA), anti-Macrophage L1 calprotectin (1:400; MAC387; Thermo Fisher Scientific Inc., Waltham, MA), anti-von Willebrand's factor (vWF) (Dako North America Inc., Carpinteria, CA), and anti-Ki67 (1:400, Thermo Fisher Scientific Inc., Waltham, MA) after heat-induced epitope retrieval when necessary. Secondary antibody detection and counterstaining were performed as described previously(9).

Image Quantification—Mosaic images of whole wounds were collected under 20× magnification guided by MosaiX software (Zeiss, Thornwood, NY) and a motorized stage. In order to cover the whole wound, each mosaic image was generated by combining a minimum of ~100 images. Between 7 and 9 high-powered representative areas from mosaic images were quantified for each time point. Image analysis was performed by employing

Auto-measure software (Zeiss) for quantitation of the percentage of immune-histochemical reaction positive areas (expressed as % area).

Laser Speckle Contrast Imaging (LASCI) Technology—PeriCam PSI System is a blood perfusion imager based on laser speckle technology. The system allows for visualization and quantification of microcirculation in tissues on a real-time basis (10). The mean blood flow was measured in excisional wounds within a 100 mm² surface area (resolution 0.54 × 0.54 mm, working distance 17-20 cm, 55 images/second).

Cell Culture, Differentiation and treatment—The human promyelocytic cells HL-60 (American Type Culture Collection [ATCC]; Manassas, VA; ATCC code CCL-240) were cultured in RPMI 1640 with L-glutamine, supplemented with 20% fetal bovine serum (FBS) and 1% penicillin-streptomycin (PS) (Gibco, Auckland, NZ). For differentiation of HL-60 cells into mature neutrophils, cells were first suspended in RPMI 1640 media, supplemented with 1% PS and 20% heat-inactivated fetal bovine serum (HIFBS) (Gibco, Auckland, NZ) followed by addition of 10 μM 13-cis-retinoic acid (Thermo Fisher, New Jersey, USA). Cultures were incubated at 37°C for 5 days. Culture media was changed every 3rd day and fresh retinoic acid was added. Human THP-1 monocytes (American Type Culture Collection, Manassas, VA) were cultured and differentiated to macrophages as described previously (11). A solution of MCG stock was prepared by dissolving 1 g of MCG per ml of culture media. To treat differentiated cells with MCG, 100 μl of MCG stock was added to culture plates containing 900 μl media.

RNA Isolation—Immediately after collection, wound tissue biopsies were rinsed in saline, patted dry and snap frozen in liquid nitrogen. Grinding of tissues was performed using 6770 Freezer/Mill® cryogenic grinder (SPEX SamplePrep, Metuchen, NJ). Total RNA from tissue or cultured cells were extracted using mirVana RNA isolation kit (Ambion, Austin, TX) as described (11, 12).

Reverse Transcription and Quantitative Real-time PCR—Tissue mRNA was quantified by real-time or quantitative (Q) PCR assay using the double-stranded DNA binding dye SYBR Green-I as described previously (12). The primer set used for the individual genes are listed below. 18s rRNA was used as a reference housekeeping gene.

Human_VEGF-A165 F: 5'-TGC CCA CTG AGG AGT CCA ACA T-3'

Human_VEGF-A165 R: 5'-CAC GTC TGC GGA TCT TGT ACA AAC A-3'

Pig_VEGF-A F: 5'-CTC TCT CTT ACT TGT ACT GGT CTT T-3'

Pig_VEGF-A R: 5'-TTA TTT CAA AGG AAT GTG TGG CG-3'

Pig_vWFF: 5'-GGC TCT GAT AAG CTG TCC GAG G-3'

Pig_vWFR: 5'-TTT CGG TCC TGG AGC GAG A-3'

Human_COL1A F: 5'-ACG TCC TGG TGA AGT TGG TC-3'

Human_COL1A R: 5'-ACC AGG GAA GCC TCT CTC TC-3'.

Enzyme-Linked Immunosorbent Assay (ELISA)—MCP-1 level in culture media was determined using commercially available ELISA kits per manufacturer's recommendation (R&D Systems, Minneapolis, MN).

Statistical Analyses

Data are reported as mean \pm SD of at least 3-4 animals as indicated. Since the data were not normally distributed, non-parametric statistics was used. The significance of differences between control and treated groups was evaluated using the two-tailed Mann-Whitney test, $p < .05$ was considered statistically significant.

RESULTS

We chose a preclinical model of full thickness dermal excisional wounds to study the effect of a modified collagen gel (MCG) on wound healing outcomes. Proteomics analysis of MCG demonstrates that Collagen (I & III), hemoglobin and peroxiredoxin are major components present in this gel formulation (Table 1). A representative mass spectrum analysis of the most abundant component of MCG, Hemoglobin subunit beta, is shown in Figure 1. This study was designed to characterize specific phases of the wound healing process by harvesting wound tissue at several time points during the course of the healing process. Specifically, we collected the wound edge tissue biopsies as shown in Figure 2A&B. Histological characterization of wound re-epithelialization was performed by staining the wound tissues for keratin-14, the type I cytokeratin that forms the cytoskeleton of epithelial cells (Fig. 2C). Tissue sections were counterstained with DAPI to visualize nuclei. Lengths of the rete ridges were measured using an automated unbiased approach by utilizing an Automeasure software (Zeiss). MCG-treated wounds displayed longer rete ridge structures compared to untreated wounds.

The wound neutrophil count on day 3 post-wounding was performed using antibody against myeloperoxidase, a lysosomal enzyme stored in azurophilic granules of the neutrophil (Fig. 3A) (13). Quantitation of MPO positive areas in mosaic images of the wound-edge tissue sections showed higher abundance of neutrophils in wounds treated with MCG (Fig. 3, B). To determine the effect of MCG on neutrophil function, we treated HL60-derived neutrophils with MCG. Such treatment significantly enhanced the release of monocyte chemoattractant protein-1 (MCP-1) by these cells (Fig. 3, C). This observation led to the hypothesis that MCG would be effective in attracting more macrophages to the wound-site *via* increased MCP-1 release. Next, macrophages were identified in wound tissue sections using antibody against the macrophage L1 protein/calprotectin (Fig. 4A), which has been reported to be a reliable marker for macrophages in swine tissue (14). The kinetics of macrophage infiltration to the excisional wound-site was evaluated over the duration of the healing process. Compared to untreated wounds, MCG-treated wounds showed significant increase in macrophage infiltration at day 3 post-wounding. Higher macrophage abundance at the MCG-treated wound-site was also noted in day 7 post-wounding. However, on day 21 post-wounding the macrophage count of MCG treated wounds reduced markedly and were comparable to that of control wounds indicating effective resolution of inflammation (Fig. 4B).

Interestingly, in studies using cultured macrophages, MCG was found to potently induce vascular endothelial growth factor (VEGF) gene expression (Fig. 4C). VEGF is a known potent angiogenic factor that is secreted into the wound tissues to promote tissue vascularization. On day 7 post-wounding, VEGF gene expression in the wound-edge tissue was noted to be significantly higher for MCG-treated wounds (Fig. 5). Consistently, abundance of endothelial cell specific gene von Willebrand's Factor (vWF) was higher in the wound-edge tissue on day 21 post-wounding. vWF is a glycoprotein that is produced by endothelial cells and is routinely used to identify vascular structures in tissue sections (Fig. 5).

During the proliferative phase of wound healing, angiogenesis is necessary to supply oxygen, nutrients and other blood-borne factors required for cell migration and proliferation. Wound tissue vascularization was evaluated through quantitative measurement of endothelial cells abundance and blood flow in pair-matched wounds. Quantitative analyses of vWF positive areas in wound sections showed significant increase of endothelial cells abundance in day 21 post-wounding tissue collected from MCG-treated wounds (Fig. 6A). Interestingly, MCG-treated wounds displayed more mature vascular formations of vWF positive cellular structures compared to untreated wounds. Functional assessment of wound tissue vascularization was accomplished by imaging blood flow using laser speckle technology *in vivo*. MCG-treatment was observed to significantly increase wound-site blood flow compared to corresponding pair-matched control wound tissue (Fig. 6B). The striking effect of MCG on wound angiogenesis led us to evaluate underlying mechanisms. Increased endothelial cell proliferation and migration are two key events that lead to enhanced angiogenesis. Thus, we studied wound-site endothelial cell proliferation using Ki67 and vWF double immune-staining followed by automated quantification of co-localized signals in the mosaic images. Ki67 is a nuclear protein that is associated with cellular proliferation (15). Marked increase of the proliferating endothelial cells was observed in MCG-treated wounds (Fig. 7).

An important aspect of the proliferative phase of wound healing is collagen deposition, which is responsible for tensile strength of the post-heal tissue. Greater tensile strength of the post-heal tissue ensures effective protection against reopening of a close wound in response to shear stress. Quantitative and qualitative analyses of collagen formation in MCG-treated or untreated wound was done using wound-edge tissue harvested on day 21 post-wounding. Initial histological examination of wound-edge tissue using Masson's Trichrome staining displayed higher abundance of mature collagen fibers in MCG-treated wounds (Fig 8A&C). Picrosirius red staining (PRS) was used to distinguish between type I and type III collagen in the wound-edge tissue (16). After staining with PRS, collagen type I (thick fibers) displays yellow-orange birefringence while type III (thin fibers) displays green birefringence when viewed under polarized light microscope. Collagen type I:III ratio was significantly increased in MCG-treated wounds compared to untreated wounds (Fig 8B&D). These histological findings were supported by measurement of collagen type I gene expression that was found to be up-regulated in MCG-treated wounds on day 14 post-wounding compared to untreated wounds (Fig. 8, E).

DISCUSSION

Collagen is the most abundant protein in mammals. In addition to being the main component of connective tissue, it is now recognized that collagen may play key role in cell signal transduction (17). Collagen induced cell signaling regulates cellular functions such as cell adhesion and migration, hemostasis, and immune function (18). Through their triple-helical regions, collagens interact with numerous signaling partners including cell surface receptors. Integrins, discoidin domain receptors, glycoprotein VI, and leukocyte-associated immunoglobulin-like receptor-1 represent some of the transmembrane receptors that recognize the collagen triple helix. Among biomaterials, the use of collagen based products is common. Biological features such as excellent biocompatibility and safety make collagen a material of choice for biomedical applications. Collagen is biodegradable and shows weak antigenicity (19). In wound care, collagen is commonly used as wound dressing material. On the practical side, collagen-based wound care dressings have the advantage of long-term storage under sterile conditions. Thus, they may be easily stockpiled for emergent needs (20). On scientific considerations, although observational studies report favorable outcomes the underlying mechanisms of action remain speculative and not established in wound healing studies. This work is the first to address such mechanisms in a pre-clinical swine

model which is known to most closely resemble the human wound (12, 21). (12, 21). Anatomically as well as physiologically, pig skin closely resembles human skin(21). Additionally, pigs and humans have similar physical and molecular responses to various growth factors (22). Thereby, the porcine model is generally accepted as an excellent tool to study wound healing.

Rete ridges are epidermal protrusions that extend downward between dermal papillae into the connective tissue of the skin. Rete ridges interlock the dermal-epidermal junction. Epidermal cells receive nutrients from the blood vessels in the dermis. Rete ridges increase the surface area of the epidermis that is exposed to these blood vessels and blood-borne nutrients. In addition, effective interlocking of the dermal-epidermal junction by rete ridges protects the skin from reopening in response to shear stress. With aging, the rete ridges are known to shorten, making the skin fragile (23, 24). Shortening of rete ridges also limits nutrient supply to the epidermis by decreasing the surface area in contact with the dermis, also interfering with the skin's normal repair process. Our observation that a collagen dressing may increase the size of rete ridges in the healing wound tissue provides first evidence demonstrating improved quality of closure, re-establishing more healthy skin featuring well-nourished epidermis, and that is potentially more resistant to re-opening of the wound in response to shear stress.

Collagen may serve as neutrophil chemotactic factor(25). Neutrophils actively migrate actively into 3-dimensional gels of collagen(26). Studies on lung injury have demonstrated that degraded collagen may support neutrophil chemotaxis(27). Consistently, we provide first evidence demonstrating that a collagen-based dressing may improve neutrophil chemotaxis into the wound-site. Neutrophils are known to be functionally activated when in contact with collagen I (28), the primary ingredient in MCG. It is therefore plausible that MCG will help the wound tissue fight infection through bolstered neutrophil function. Monocyte chemotactic protein-1 (MCP-1) or chemokine (C-C motif) ligand 2 (CCL2) is a major driver of wound inflammation. Neutrophil derived MCP-1 play a key role in recruiting macrophages to the wound-site(29). In addition to our observation that MCG recruits larger number of neutrophils to the wound site we noted that in neutrophil-like differentiated HL60 cells MCG induced MCP-1 expression. This would suggest that *via*its activity on wound-site neutrophils, MCG would be able to mount a more inflammatory response by recruiting more macrophages to the wound-site. Macrophages are beneficial to wound healing as long as inflammation resolves in a timely manner and does not end up being chronic (30). Analysis of the wound-edge tissue at multiple time-points following wounding demonstrated that MCG potently bolstered recruitment of macrophages to wound site. Importantly, such effect was accompanied with efficient resolution of inflammation as shown by the rapid return of macrophage count to control values. Taken together, MCG strengthened the inflammatory response following wounding by supporting neutrophil and macrophage chemotaxis.

Inflammation is widely recognized to be a major driver of angiogenesis. Peripheral blood monocyte subsets recruited into the wound-site promote wound tissue vascularization (31). At the wound-site, macrophages produce VEGF which in turn supports endothelial cell proliferation(32). We noted induction of VEGF expression in the wound-edge tissue of MCG treated wounds. Consistently, we noted higher abundance of von Willebrand Factor gene, a marker of endothelial cell in such treated wounds. Higher abundance of endothelial cells in MCG treated wound-edge tissue was confirmed using immunohistochemical studies to detect endothelial cells. Endothelial cell proliferation, known to be induced by extracellular matrix component such as collagen, represents a major component of angiogenesis (33, 34). Immunohistochemical studies demonstrated that in wound tissue treated with MCG, endothelial cell proliferation was significantly higher. To test the

functional significance of a higher abundance of endothelial cells at the MCG treated wound-site, blood flow imaging was performed using a laser speckle contrast imaging system. The laser speckle contrast imaging is a high-resolution and high contrast optical imaging technique often used to image blood flow dynamics in real time with excellent spatial and temporal resolution (35). Quantitative analysis of blood flow established that MCG treatment significantly improved blood flow to the wound tissue.

During the later remodeling stage of wound healing, appropriate collagen deposition is important because it increases the strength of the wound tissue resisting reopening caused by shear stress. In addition, it provides appropriate signaling cues to cells at the wound site to complete the healing process. We observed significantly increased collagen deposition during the later stages of MCG treated wounds. Types I and III collagen are fibril forming interstitial collagens most abundant in the skin. Collagen type III (thin fibers) is laid down first early after injury which supports the healing wound until it is replaced by stronger collagen type I (thick fibers) late during maturation (36). Increased collagen type I:III ratio is crucial for tensile strength of healing wounds(37, 38). Several clinical studies have reported that decreased collagen I:III ratio was associated with post-operative recurrence of incisional hernia through surgical wounds(39). Also, impaired biomechanical properties of diabetic skin was associated with lowered collagen I and collagen I:III ratio (40). This explains the compromised mechanical stability of diabetic wounds to withstand traumatic injury. In this current work, MCG treatment significantly increased collagen I:III ratio on day 21 post-wounding. In support of this observation we noted that MCG induced the expression of type I collagen gene demonstrating host skin response to the applied collagen dressing. Elongated rete ridges and elevated collagen I:III ratio predicts improved ability of the MCG treated wound to withstand shear stress and reopening.

In summary, the study presents first evidence from a pre-clinical setting explaining how a collagen based dressing may improve wound closure by targeting multiple key mechanisms including a more robust transient inflammatory response followed by improved wound tissue vascularization and collagen deposition. The current findings warrant additional studies to determine whether the responses to the MCG are different from other modified or unmodified collagen based products used in clinical setting.

Acknowledgments

We thank Prashant Sinha, MD and Jennifer Dickerson, RVT for assistance with the conduct of experiments. The work was supported by National Institutes of Health awards GM077185, GM069589 and DK076566. We thank Dr. Ed Stout and Ms. Angie McKessor Southwest Technologies for providing the dressing and unrestricted research development funding to The Ohio State University.

REFERENCES

1. Moulik PK, Mtonga R, Gill GV. Amputation and mortality in new-onset diabetic foot ulcers stratified by etiology. *Diabetes Care*. 2003; 26(2):491–4. [PubMed: 12547887]
2. Sen CK, Gordillo GM, Roy S, Kirsner R, Lambert L, Hunt TK, et al. Human skin wounds: a major and snowballing threat to public health and the economy. *Wound Repair Regen*. 2009; 17(6):763–71. [PubMed: 19903300]
3. Schultz GS, Wysocki A. Interactions between extracellular matrix and growth factors in wound healing. *Wound Repair Regen*. 2009; 17(2):153–62. [PubMed: 19320882]
4. Akturk O, Tezcaner A, Bilgili H, Deveci MS, Gecit MR, Keskin D. Evaluation of sericin/collagen membranes as prospective wound dressing biomaterial. *J Biosci Bioeng*. 2011; 112(3):279–88. [PubMed: 21697006]

5. Metzmacher I, Ruth P, Abel M, Friess W. In vitro binding of matrix metalloproteinase-2 (MMP-2), MMP-9, and bacterial collagenase on collagenous wound dressings. *Wound Repair Regen.* 2007; 15(4):549–55. [PubMed: 17650099]
6. Brett D. Review of collagen and collagen-based wound dressings. *WOUNDS.* 2008; 20(12):347–53.
7. Luzio, P.; Paludo, P. Chronic leg ulcer treated with collagen and glycerine-based dressing. Proceedings of the European Wound Management Association; Lisbon, Portugal. 2008 May 14th-16th;
8. Filho, JM.; Leal, F. Use of new collagen and/or glycerine dressings in complex dermatology surgery procedures like Mohs surgery, tumor excision and others. Proceedings of the Symposium on Advanced Wound Care & Wound Healing Society; Tampa, Florida. 2007 April 28th - May 1st;
9. Roy S, Khanna S, Nallu K, Hunt TK, Sen CK. Dermal wound healing is subject to redox control. *Mol Ther.* 2006; 13(1):211–20. [PubMed: 16126008]
10. Choi B, Ramirez-San-Juan JC, Lotfi J, Stuart Nelson J. Linear response range characterization and in vivo application of laser speckle imaging of blood flow dynamics. *J Biomed Opt.* 2006; 11(4): 041129. [PubMed: 16965157]
11. Ganesh K, Das A, Dickerson R, Khanna S, Parinandi NL, Gordillo GM, et al. Prostaglandin E2 Induces Oncostatin M Expression in Human Chronic Wound macrophages through Axl Receptor Kinase Pathway. *J Immunol.* 2012 in Press.
12. Roy S, Biswas S, Khanna S, Gordillo G, Bergdall V, Green J, et al. Characterization of a preclinical model of chronic ischemic wound. *Physiol Genomics.* 2009; 37(3):211–24. [PubMed: 19293328]
13. Klebanoff SJ. Myeloperoxidase: friend and foe. *J Leukoc Biol.* 2005; 77(5):598–625. [PubMed: 15689384]
14. Dor FJ, Gollackner B, Kuwaki K, Ko DS, Cooper DK, Houser SL. Histopathology of spleen allograft rejection in miniature swine. *Int J Exp Pathol.* 2005; 86(1):57–66. [PubMed: 15676033]
15. Gerdes J, Lemke H, Baisch H, Wacker HH, Schwab U, Stein H. Cell cycle analysis of a cell proliferation-associated human nuclear antigen defined by the monoclonal antibody Ki-67. *J Immunol.* 1984; 133(4):1710–5. [PubMed: 6206131]
16. Montes GS, Junqueira LC. The use of the Picosirius-polarization method for the study of the biopathology of collagen. *Mem Inst Oswaldo Cruz.* 1991; 86(Suppl 3):1–11. [PubMed: 1726969]
17. Vogel WF. Collagen-receptor signaling in health and disease. *Eur J Dermatol.* 2001; 11(6):506–14. [PubMed: 11701397]
18. Leitinger B. Transmembrane collagen receptors. *Annu Rev Cell Dev Biol.* 2011; 27:265–90. [PubMed: 21568710]
19. Lee CH, Singla A, Lee Y. Biomedical applications of collagen. *Int J Pharm.* 2001; 221(1-2):1–22. [PubMed: 11397563]
20. Benjamin HB, Pawlowski E, Becker AB. Collagen as temporary dressing and blood vessel replacement. *Arch Surg.* 1964; 88:725–7. [PubMed: 14120696]
21. Sullivan TP, Eaglstein WH, Davis SC, Mertz P. The pig as a model for human wound healing. *Wound Repair Regen.* 2001; 9(2):66–76. [PubMed: 11350644]
22. Broughton G 2nd, Janis JE, Attinger CE. The basic science of wound healing. *Plast Reconstr Surg.* 2006; 117(7 Suppl):12S–34S. [PubMed: 16799372]
23. Naylor EC, Watson RE, Sherratt MJ. Molecular aspects of skin ageing. *Maturitas.* 2011; 69(3): 249–56. [PubMed: 21612880]
24. Gilchrist BA. A review of skin ageing and its medical therapy. *Br J Dermatol.* 1996; 135(6):867–75. [PubMed: 8977705]
25. Nakagawa H, Takano K, Kuzumaki H. A 16-kDa fragment of collagen type XIV is a novel neutrophil chemotactic factor purified from rat granulation tissue. *Biochem Biophys Res Commun.* 1999; 256(3):642–5. [PubMed: 10080952]
26. Islam LN, McKay IC, Wilkinson PC. The use of collagen or fibrin gels for the assay of human neutrophil chemotaxis. *J Immunol Methods.* 1985; 85(1):137–51. [PubMed: 4078307]

27. Riley DJ, Berg RA, Soltys RA, Kerr JS, Guss HN, Curran SF, et al. Neutrophil response following intratracheal instillation of collagen peptides into rat lungs. *Exp Lung Res.* 1988; 14(4):549–63. [PubMed: 3208719]
28. Monboisse JC, Garnotel R, Randoux A, Dufer J, Borel JP. Adhesion of human neutrophils to and activation by type-I collagen involving a beta 2 integrin. *J Leukoc Biol.* 1991; 50(4):373–80. [PubMed: 1680954]
29. Miyazaki S, Matsukawa A, Ohkawara S, Takagi K, Yoshinaga M. Neutrophil infiltration as a crucial step for monocyte chemoattractant protein (MCP)-1 to attract monocytes in lipopolysaccharide-induced arthritis in rabbits. *Inflamm Res.* 2000; 49(12):673–8. [PubMed: 11211917]
30. Khanna S, Biswas S, Shang Y, Collard E, Azad A, Kauh C, et al. Macrophage dysfunction impairs resolution of inflammation in the wounds of diabetic mice. *PLoS One.* 2010; 5(3):e9539. [PubMed: 20209061]
31. Willenborg S, Lucas T, van Loo G, Knipper JA, Krieg T, Haase I, et al. CCR2 recruits an inflammatory macrophage subpopulation critical for angiogenesis in tissue repair. *Blood.* 2012
32. Cho M, Hunt TK, Hussain MZ. Hydrogen peroxide stimulates macrophage vascular endothelial growth factor release. *Am J Physiol Heart Circ Physiol.* 2001; 280(5):H2357–63. [PubMed: 11299242]
33. Roy S, Driggs J, Elgharably H, Biswas S, Findley M, Khanna S, et al. Platelet-rich fibrin matrix improves wound angiogenesis via inducing endothelial cell proliferation. *Wound Repair Regen.* 2011; 19(6):753–66. [PubMed: 22092846]
34. Browne CD, Hindmarsh EJ, Smith JW. Inhibition of endothelial cell proliferation and angiogenesis by orlistat, a fatty acid synthase inhibitor. *FASEB J.* 2006; 20(12):2027–35. [PubMed: 17012255]
35. Dunn AK. Laser speckle contrast imaging of cerebral blood flow. *Ann Biomed Eng.* 2012; 40(2): 367–77. [PubMed: 22109805]
36. Stadelmann WK, Digenis AG, Tobin GR. Physiology and healing dynamics of chronic cutaneous wounds. *Am J Surg.* 1998; 176(2A Suppl):26S–38S. [PubMed: 9777970]
37. Hurme T, Kalimo H, Sandberg M, Lehto M, Vuorio E. Localization of type I and III collagen and fibronectin production in injured gastrocnemius muscle. *Lab Invest.* 1991; 64(1):76–84. [PubMed: 1703587]
38. Dale PD, Sherratt JA, Maini PK. A mathematical model for collagen fibre formation during foetal and adult dermal wound healing. *Proc Biol Sci.* 1996; 263(1370):653–60. [PubMed: 8677263]
39. Junge K, Klinge U, Rosch R, Mertens PR, Kirch J, Klosterhalfen B, et al. Decreased collagen type I/III ratio in patients with recurring hernia after implantation of alloplastic prostheses. *Langenbecks Arch Surg.* 2004; 389(1):17–22. [PubMed: 14576942]
40. Bermudez DM, Herdrich BJ, Xu J, Lind R, Beason DP, Mitchell ME, et al. Impaired biomechanical properties of diabetic skin implications in pathogenesis of diabetic wound complications. *Am J Pathol.* 2011; 178(5):2215–23. [PubMed: 21514435]

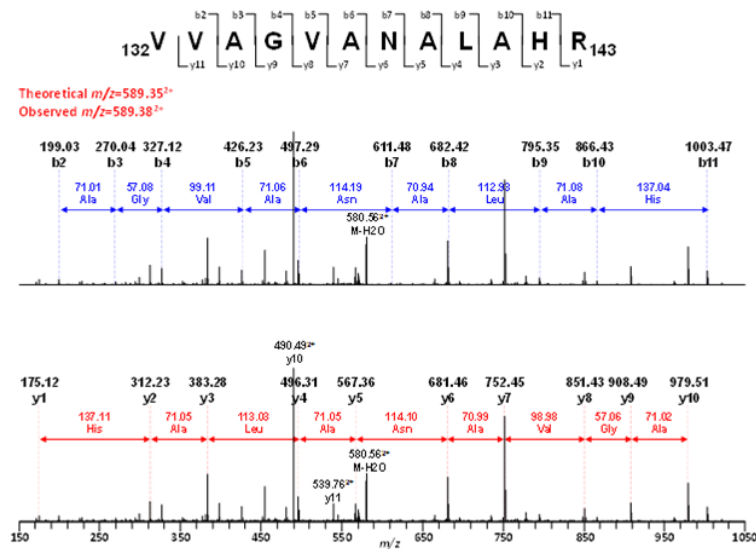


Figure 1. Representative MS/MS spectrum of peptide 132VVAGVANALAH R143 from Hemoglobin subunit beta (bovine)

The scan sequence of the mass spectrometer was based on the TopTen™ method; the analysis was programmed for a full scan recorded between 350 – 2000 Da, and a MS/MS scan to generate product ion spectra to determine amino acid sequence in consecutive instrument scans of the ten most abundant peak in the spectrum. Protein identifications were checked manually and proteins with a Mascot score of 50 or higher with a minimum of two unique peptides from one protein having a *-b* or *-y* ion sequence tag of five residues or better were accepted.

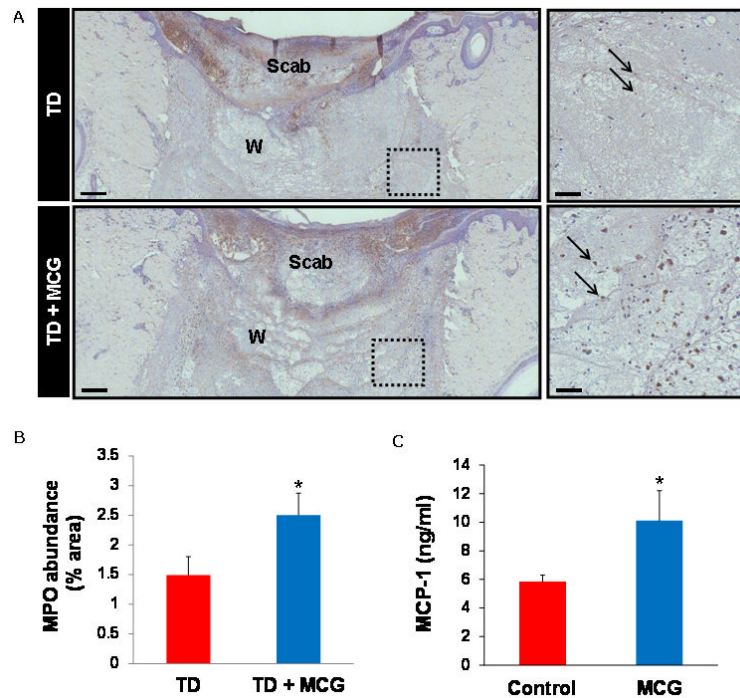


Figure 2. Experiment design and wound re-epithelialization

(A) Four sets with 8 excisional 3 mm punch wounds in each set were created on each side of the back of pigs ($n = 4$). One set of 8 wounds were collected at specified time points (days 3-21) post wounding. (B) Wounds on one side of the back were either treated with a modified collagen gel (MCG), followed by covering with Tegaderm™ (TD) or TD alone (control, contralateral side) (C) Representative images showing increased length of rete ridges in the MCG treated excisional wounds on day 7 post wounding. OCT embedded frozen wound biopsies were sectioned ($8 \mu\text{m}$) and stained using anti-keratin-14 (K14, green) and DAPI (blue) immune-fluorescence staining. The arrows indicate the two edges of the wound. Bar graph presents the length of rete ridges within wound as quantified using MosaiX software (Zeiss). Scale bar, $500 \mu\text{m}$. Data are mean \pm SD ($n = 4$); * $p < 0.05$ compared to untreated control wounds.

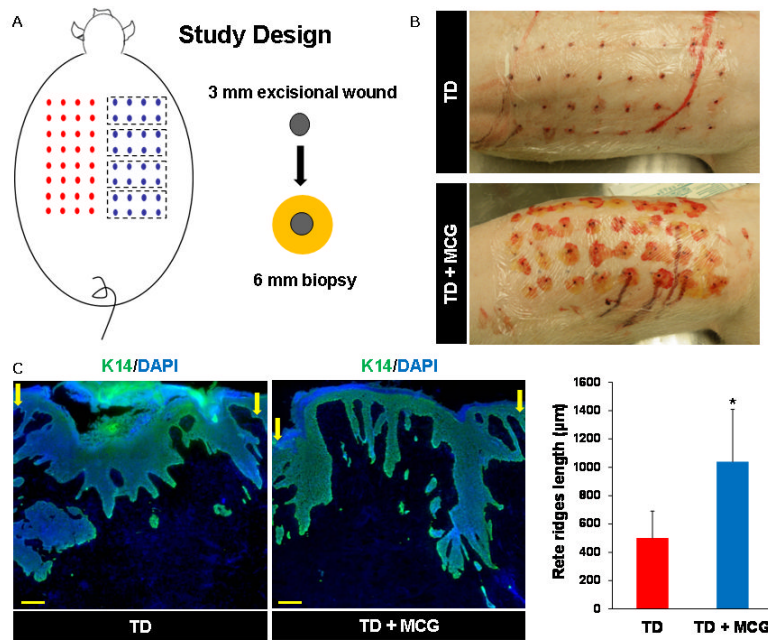


Figure 3. Increased neutrophil infiltration in excisional wounds treated with modified collagen gel (MCG)

(A) Formalin-fixed paraffin-embedded (FFPE) wound biopsies were resectioned ($5 \mu\text{m}$) and stained using anti-myeloperoxidase (MPO, dark brown). The sections were counterstained with hematoxylin (blue). Scale bar, 1 mm. W, wound; TD, TegadermTM; MCG, modified collagen gel. Right panels are the zoom of the boxed area of images shown in left panels. Scale bar, $100 \mu\text{m}$. (B) Bar graph shows quantitation of neutrophils at day 3 post-wounding in MCG-treated or -untreated control excisional wounds. Data are presented as mean \pm SD ($n = 4$); $*p < 0.05$ compared to untreated wounds. (C) Release of monocyte chemoattractant protein-1 (MCP-1) from HL60-derived human neutrophils treated with modified collagen gel (MCG). HL60 cells were differentiated into neutrophils and incubated for 24h with or without MCG. MCP-1 concentration in media was measured using enzyme-linked immunosorbent assay. Data are mean \pm SD ($n = 4$); $*p < 0.05$ compared to untreated cells.

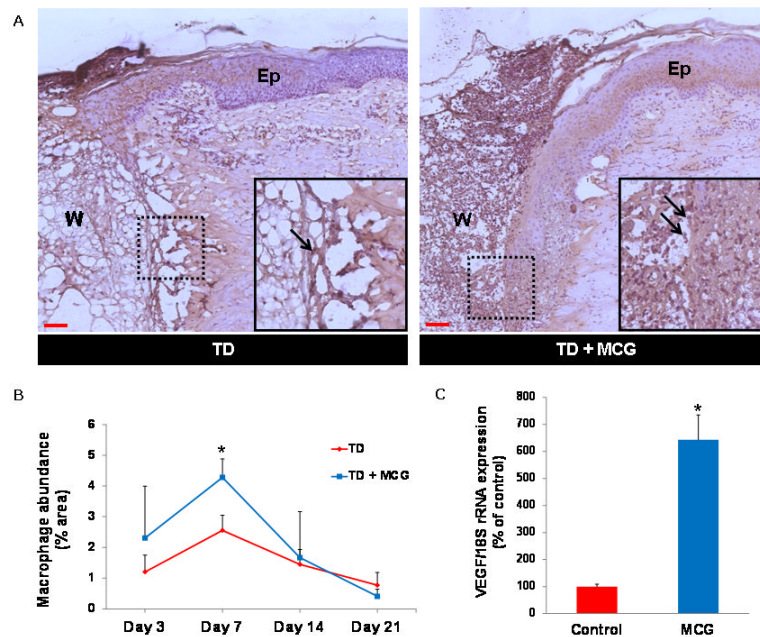


Figure 4. Increased macrophages infiltration in excisional wounds treated with modified collagen gel (MCG)

(A) Representative images from formalin-fixed paraffin-embedded biopsy tissue sections (5 μm) that were immunostained using macrophage/calprotectin specific antibody (dark brown). The sections were counterstained with hematoxylin (blue). Scale bar, 500 μm . Insets are the zoom of the dashed box areas in the image. Ep, epidermis; W, wound; TD, TegadermTM, MCG, modified collagen gel. (B) Bar graph shows quantitation of the kinetics of macrophage infiltration in MCG-treated or control wounds. Data are presented as mean \pm SD ($n = 3$); * $p < 0.05$ compared to untreated wounds. (C) Vascular endothelial growth factor (VEGF) gene expression in THP-1 differentiated human macrophages treated with modified collagen gel (MCG) for 24h. VEGF gene expression was measured using quantitative real-time PCR. Data are presented as % change compared to untreated cells. Data are mean \pm SD ($n = 4$); * $p < 0.05$.

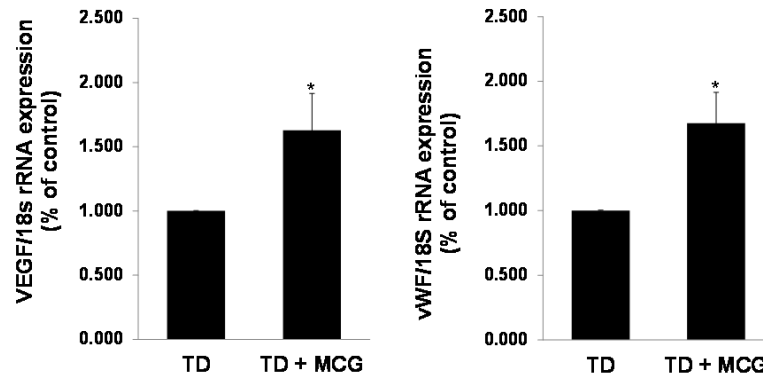


Figure 5. Up-regulation of vascular endothelial growth factor (VEGF) and von Willebrand Factor (vWF) genes expression in excisional wounds treated with modified collagen gel (MCG) Total RNA was isolated from wound biopsy tissue material stored in liquid nitrogen. Real-time PCR was used to measure: (A) VEGF gene expression in day 7 post-wound tissues and (B) vWF gene expression in day 21 post-wound tissues. Gene expression data are presented as % change compared to untreated control wound tissues. Data are mean \pm SD ($n = 4$); * $p < 0.05$.

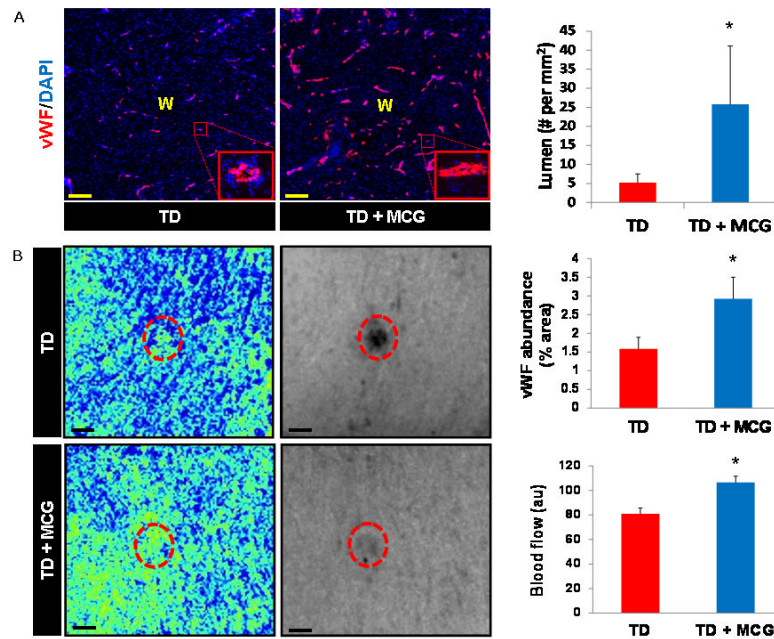


Figure 6. Increased vascularization in excisional wounds treated with modified collagen gel (MCG)

(A) Representative immunofluorescence images from wound sections (8 μm) stained using von Willebrand Factor (red) and DAPI (blue). Inset shows the lumen like structure counted for the adjacent quantitative graph presented. Scale bar, 50 μm . Bar graphs (top and middle) shows quantitation of the lumen like structures in each group (top bar graph) and endothelial cell in MCG-treated or untreated excisional wounds day 21 post-wounding (middle bar graph). Data are presented as mean \pm SD ($n = 3$); * $p < 0.05$ compared to untreated wounds. W, wound area; TD, Tegaderm™; MCG, modified collagen gel. (B) Laser Speckle images of MCG treated or control excisional wounds on day 21 post-wounding. Left panels are speckle flow color images (yellowish-green color represents increased blood flow) while right panels are black/white contrast images (red dashed circles indicate the site of excisional wounds). Scale bar, 2.4 mm. Bar graph (bottom) represents the quantitative data from Laser Speckle analysis. Data presented as mean \pm SD ($n = 4$); * $p < 0.05$ compared to untreated wounds.

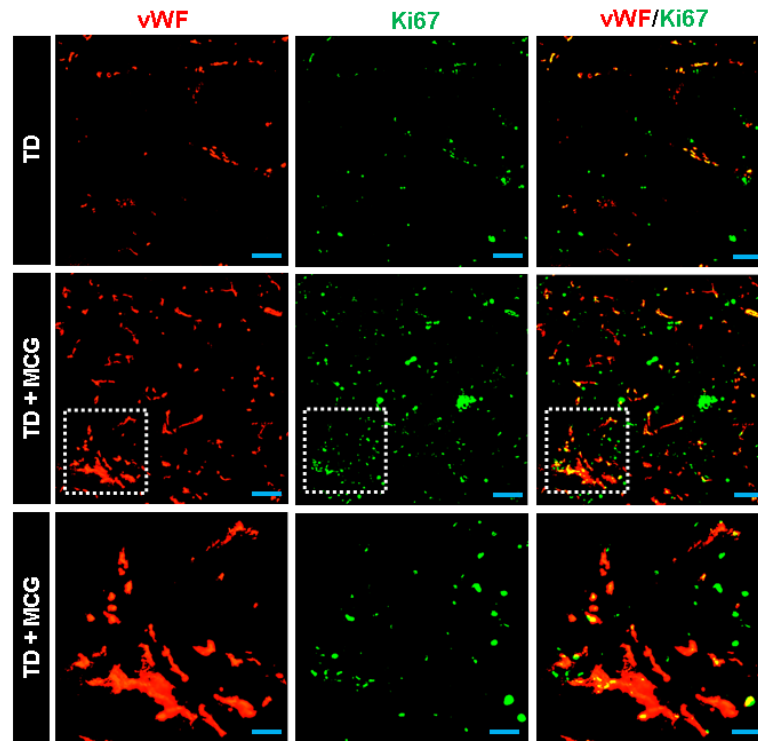


Figure 7. Increased proliferation of wound endothelial cells in modified collagen gel (MCG) treated wounds

Representative immunofluorescence images of wound sections (8 μm) stained using Ki67 (marker of proliferating cells, green) and von Willebrand Factor (endothelial cells, red). Compared to untreated excisional wounds, the MCG-treated wounds showed increased number of vWF-positive proliferating cells (yellow areas in merged images). The bottom panels are zoom of dashed white box in middle panels. Top and middle panels scale bars, 100 μm . Bottom panel scale bar, 20 μm .

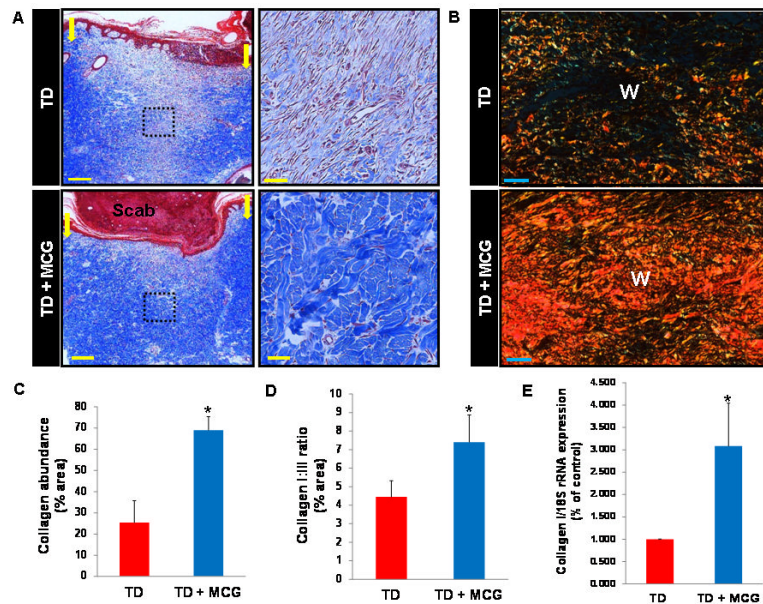


Figure 8. Increased collagen abundance in excisional wounds treated with modified collagen gel (MCG)

(A) Representative images of formalin-fixed paraffin-embedded (FFPE) wound biopsy sections (5 μ m) stained using Masson's Trichrome staining. This staining results in blue-black nuclei, blue collagen, and light red or pink cytoplasm cytoplasm. Epidermal cells appear reddish. Scale bar, 500 μ m. The arrows indicate the edges of the wound. Right panels are the zoom of boxed area of images shown in left panel. Scale bar, 50 μ m. (B) Representative images from FFPE wound tissue biopsy sections stained using picrosirius red staining (PRS). This stain can be used to distinguish between type I and type III collagen in wound tissues; type I (thick fibers) appears yellow-orange birefringence while type III (thin fibers) appears green birefringence when viewed under polarized light microscope. (C) Bar graph shows quantitation of collagen abundance in MCG-treated or -untreated control woundson day 21 post-wounding. Data are presented as mean \pm SD ($n = 3$); $*p < 0.05$ compared to untreated wounds. W, wound. (D) Bar graph shows quantitation of the ratio of collagen types-I & -III. Scale bar, 75 μ m. Data are mean \pm standard deviation ($n = 3$); $*p < 0.05$ compared to untreated control wounds. (E) Collagen type I gene expression in excisional wounds treated with modified collagen gel (MCG). The collagen type I gene expression in day 14 wound tissues was quantified using real-time PCR. Gene expression data are presented as % change compared to MCG-untreated control wound tissues. Data are mean \pm SD ($n = 4$); $*p < 0.05$.

Table 1

Proteomic analysis of MeG components *

Sl. No	Description	Accession	Unigene ID	Mass (Da)	Number of significant sequences	Score
1	Hemoglobin subunit beta **	HBB_BOVIN	Bt.23726	16001	7	685
2	Carbonic anhydrase 2	CAH2_BOVIN	Bt.49731	29096	10	650
3	Collagen alpha-1 (I) chain	CO1A1_BOVIN	Bt.23316	139880	3	321
4	Hemoglobin subunit alpha	HBA_BOVIN	Bt.10591	15175	5	319
5	Peroxire doxin-2	PRDX2_BOVIN	Bt.2689	22217	5	308
6	Alpha-1-antiproteinase	A1AT_BOVIN	Bt.982	46417	2	220
7	Serpin A3-7	SPA37_BOVIN	Bt.55387 Bt.92049	47140	3	161
8	Collagen alpha-1(III) chain	CO3A1_BOVIN	Bt.64714	93708	2	147
9	Collagen alpha-2(I) chain	CO1A2_BOVIN	Bt.53485	129499	2	103
10	Serpin A3-3	SPA33_BOVIN	Bt.55387 Bt.92049	46411	2	85
11	Actin, aortic smooth muscle	ACTA_BOVIN	Bt.37349	42381	2	79

* Top ten most abundant proteins as detected using proteomics analysis has been presented Two unique peptides from one protein haloing a -b or -y ion sequence tag of five residues or better were accepted.

** Representative Mass spectrum shown in figure 1